Manuscript
Click here to access/download;Manuscript;paper_revision - Final.tex
Click here to view linked References

Noname manuscript No.
(will be inserted by the editor)

Financial interbanking networks resilience under shocks propagation

Roy Cerqueti · Matteo Cinelli · Giovanna Ferraro · Antonio Iovanella

Received: date / Accepted: date

Abstract The concept of resilience – i.e., the ability of a unified structure to absorb shocks – is of high relevance in the context of network modelling and analysis, mainly when referred to finance. This paper starts from this premise, and deals with the resilience of a financial interbanking system. At this aim, we firstly introduce a new measure of the resilience of a network, by taking into full consideration the influence of the topology of the network and the weights of its links in the shocks propagation; then, we build one financial network model related to the quarterly-based interbanking sector, whose weights are calibrated on high quality empirical data; lastly, we compute the resilience measure of the considered networks. A discussion of the results is provided, by considering both finance and network theory perspectives.

Roy Cerqueti (http://orcid.org/0000-0002-1871-7371)
Department of Social and Economic Sciences
Sapienza University of Rome
P.le A. Moro, 5 - 00185 Rome, Italy
E-mail: roy.cerqueti@uniroma1.it

Matteo Cinelli (http://orcid.org/0000-0003-3899-4592)
Department of Computer Science
Sapienza University of Rome
Viale Regina Elena, 295 — 00161 Rome, Italy
Italian National Research Council — Institute for Complex Systems
Via dei Taurini 19 - 00185, Rome, Italy
E-mail: matteo.cinelli@uniroma1.it

Giovanna Ferraro (http://orcid.org/0000-0003-4053-7649)
Department of Engineering and Architecture
University of Parma
Parco Area delle Scienze, 181/A - 43124 Parma, Italy
E-mail: giovanna.ferraro@unipr.it

Antonio Iovanella, corresponding author (http://orcid.org/0000-0001-8147-3747)
School of Economics
University of International Studies of Rome - UNINT,
Via Cristoforo Colombo, 200 - 00147 Rome, Italy
E-mail: antonio.iovanella@unint.eu

Keywords Financial interbanking networks · Network modelling and analysis · Resilience · Shock propagation · Interconnectedness · Bank for International Settlements

1 Introduction

Assessing the ability of a system to absorb shocks is a very relevant task. Indeed, it is not rare to assist at macroscopic fluctuations of a complex system generated by a microscopic impulse occurring in one of its components. The consequences of such sources of instability might be devastating; hence, their prevention and management represent targets for all the actors operating around the observed system.

From this perspective, the high attention paid to the resilience is considered useful in order to acquire insights concerning complex systems and, in particular, complex networks. Starting from the seminal paper of Albert et al. [2], resilience in complex networks was investigated theoretically [22] and then extended by considering the effects of different node removal strategies on the network structure ([20], [27]) or as a function of nodes' mixing preferences [15].

For the special theme of the resilience, it is natural to capture the propagation of a shock over a system as a transition from different sites through their connecting links. In the scientific literature, the study of the resilience is mainly related to the analysis of a performance measure, typically the diameter of the network, under two different schemes of stress depending on a targeted attack to a particular node or considering the random failure of a node, viewed as a network error ([2], [10]). Such analysis are relatively easy to perform and this explains why the models of resilience of a system are framed in the context of complex networks [20].

In this paper, the assessment of the resilience is performed by taking into considerations a new measure based on the shocks occurring in one of the nodes and on its propagation over the links of the network. We assume that the propagation of a shock from a node to another one occurs over the shortest path connecting the nodes. In so doing, we develop a model where the nodes are immunized from the subsequent effects of the shock, once they are infected for the first time by its propagation. This condition is particularly reasonable in several real-world situations. Moreover, it offers also relevant advantages under the perspective of the computational complexity of the applications of such a resilience measure. Indeed, under a purely methodological point of view, the considered resilience measure is similar to that presented in [9], by overcoming its limitations in terms of its applicability opportunities when focusing on the shortest paths. Indeed, as indicated in [12], the computation time of all simple paths grows exponentially with the size of the network [21], thus only small networks can be analysed in an acceptable time. Importantly, in line with [9], we assume that the propagation of the shock is opportunely rescaled as the distance from the shocked nodes increases. In doing so, we provide a versatile device which includes either amplified or dampened effects of the distance from the shocked node – where the nature of the effects has to be identified on the basis of the considered real world case. In this context, a relevant role is played by the identification of the size of the shock (on this, see also [1]).

The proposed resilience measure shows some clear advantages with respect to the existing ones. Indeed, we point out that the most popular resilience measure

in the environment of complex networks is based on the nodes removal, with the assessment of the reaction of the overall system to such an impulsive shock (see [2]). Under a different perspective, we can also consider resilience measures based on a cascade model (see e.g. [36] and [37]). In such a context, the failure of a node generates an avalanche-like event that may generate the disruption of the entire system. Such measures are not suitable to provide a proper modelling of our framework. Indeed, a resilience measure based on nodes removal is not a reliable device in a context such as the financial one – where the actors go in distress but are not removed from the system; furthermore, cascade-based models are associated to collapsing systems, while here we discuss the direct reaction of the single nodes to the shocks propagating from other nodes. In this respect, the resilience measure proposed in our paper is suitable for financial applications, in that it includes also the propagation of the financial distress from a country to another one.

As we will see, the methodological proposal is tested over a relevant financial network associated to the interbanking sector. The motivations for this choice lies in the paradigmatic relevance of the financial context, mainly when one deals with the concept of resilience. In fact, accounting for shocks propagation in finance contributes to describe a pivotal feature of financial systems, which has been tested by several paradigmatic cases such as the financial contagion associated to the Lehman Brothers' bankruptcy [18]. This explains why in the wide world of complex networks, those of financial nature are of particular interest [3]. Many applications were studied considering dynamic evolution [33], incomplete information [13], risk management [30] and diffusion of contagion and its relationship with the network structure ([19], [24]). Indeed, the constitutive property of a network model – i.e., the presence of disaggregated units which are mutually interconnected – is crucial when the aim is to describe financial patterns (see e.g. [32] or the review in [34]).

In detail, we propose a complex network model for the interbanking sector, where nodes are countries and links are weighted on the basis of the mutual exposures among the banks headquartered in the countries. Specifically, we hypothesize that the stronger the mutual exposures among the banks, the higher the weights of the links among the related countries, as intuitively should be.

Following previous contributions in the quantitative finance literature, we have retrieved the empirical quarterly data from the Bank for International Settlements (BIS) database (see e.g. [7], [8], [13], [17], [23], [29] and [28]). The BIS is owned by 62 central banks covering about 95% of the world's GDP [6]. The analysis is carried out also at a temporal level. The period under investigation is 2005-2020 (this latter limited to the first two quarters); such a multiperiodal framework leads to a deep analysis of the resilience evolution in the considered network, in that we build a network for each quarter of the investigated period. Moreover, the financial crisis due to Lehman Brothers' failure [18] is also taken into consideration.

It is also important to notice that BIS networks are not small enough to face the computational complexity associated to the computation of the resilience measure when not restricting to the shortest paths. However, we point out that such an approximation is quite reasonable in our specific context, since it describes the real situation of a financial contagion walking over the easiest and most direct propagation patterns (see the discussion on this point in the monograph [11]). In this respect, our methodological proposal is also able to model the real world

situation where a node is infected only once – hence, through the shortest paths – and does not react to subsequent solicitations stemming from the same shocks.

Results on the BIS networks offer a complete view of the considered interbanking sector over the period under investigation. In particular, we observe different resilience patterns as time goes from 2005 to 2020 which significantly correlate with the recorded financial history of such years.

Interestingly, the action of the amplifying/dampening effect of the shocks as the distance from the shocked node increases is relevant. Moreover, there is a reasonable dependence of the resilience of the network on the size of the shock. The obtained outcomes state clearly that large interbank exposures lead to a high level of resilience. In this respect, the years related to the recent economic distresses – the Lehman Brothers' bankruptcy in 2008 and the COVID-19 pandemic in 2020 – are associated to resilience peaks, in agreement with the stylized fact that correlation among banks increases in situations of financial distress.

The paper is organised as follows. Section 2 introduces the resilience measure used in our analysis, by including also a discussion related to the complexity of the considered tool. Section 3 outlines the proposed interbanking network model. Section 4 reports the results of the simulations performed and the related discussions. Finally, Section 5 offers some conclusive remarks and outlines directions for future research.

2 The resilience measure

Herein, we introduce the measure of resilience that we will use in the analyses as well as the rationale behind the construction of such a measure. At this aim, as we will see in detail below, we start from [9] and remove the limitations of the resilience measure in the quoted paper related on its computational complexity – hence, preventing to its applicability in contexts of highly dense networks.

We consider a set $V = \{1, \dots, n\}$, representing the set of the nodes of a complex directed and weighted network.
The adjacency matrix of the network is denoted by $\mathbf{W} = (w_{ij})_{i,j \in V}$. Matrix $\mathbf{W}$ is not necessarily symmetric.

We assume that $w_{ij} > 0$ if and only if there exists a directed link between nodes i and j. In doing so, the adjacency matrix $\mathbf{W}$ provides a straightforward identification of the links connecting the nodes of the network. When needed, we refer to E as the set of the links of the network.

We now give an integer $k \geq 2$ and introduce the k-paths with starting node $i_0 \in V$ by $p_{i_0}^{(k)} = \{i_0 \to i_1 \to \cdots \to i_{k-1} \to i_k\}$, with $i_0, i_1, \dots, i_{k-1}, i_k$ distinct nodes in V and $i_{h-1} \to i_h \in E$, for each $h = 1, \dots, k$. The node i_k is said to be the terminal node of $p_{i_0}^{(k)}$. When needed, we will refer to $p_{i_0,i_k}^{(k)}$ to specify both the initial node and the terminal node.

Intuitively, the (aggregate) weight of a generic k-path starting from i_0 and with terminal node i_k is

$$w(p_{i_0,i_k}^{(k)}) = \sum_{h=1}^{k} w_{i_{h-1} i_h}. \tag{1}$$

We assume that the diameter of the network is $\bar{k}$, so that $k = 2, \dots, \bar{k}$.

All the k-paths of the network are collected in

$$\mathcal{P}^{(k)} = \bigcup_{i_0 \in V} \mathcal{P}^{(k)}(i_0), \tag{2}$$

where $\mathcal{P}^{(k)}(i_0)$ is the collection of the k-paths whose starting node is i_0.

The set $\mathcal{P}^{(k)}$ in (2) can be quite large, mainly when the considered network is dense and it has a large number of nodes. Indeed, given two nodes $i_0, i_k \in V$, one can have a large number of different paths starting from i_0 and with terminal node i_k. Such an evidence is the ground of the computational complexity arising in the resilience measure proposed by [9].

For this reason, we conveniently restrict our attention to a special subset of $\mathcal{P}^{(k)}$.

At this aim, given two nodes $i_0, i_k \in V$, we introduce the shortest path with starting point i_0 and terminal point i_k as

$$p^{min}_{i_0,i_k} = \text{argmin} \left\{ w(p_{i_0,i_k}) : p_{i_0,i_k} \in \bigcup_{h=1}^{\bar{k}} \mathcal{P}^{(k)} \right\}. \tag{3}$$

Evidently, formula (3) entails that the shortest path with initial value i_0 and terminal value i_k is not necessarily unique. Therefore, once i_0 and i_k are fixed, being a shortest path connecting i_0 with i_k is an equivalence relation. Thus, we can identify the equivalence class collecting the shortest paths from i_0 to i_k, namely $[p^{min}_{i_0,i_k}]$. Hereafter, we will consider only one element of each equivalence class $[p^{min}_{i_0,i_k}]$, without duplicating the shortest paths associated to the same couple of nodes. We denote the representative element of $[p^{min}_{i_0,i_k}]$ as $p^{min}_{i_0,i_k}$, and we refer to it simply as shortest path from i_0 to i_k. All the shortest paths of the network – clearly, to be intended in the sense of the representative elements – are collected in a set $\mathcal{P}_{short}$.

We are now in the position of defining the shocks, which are here local events occurring to the nodes of the network. The entity of the shock plays a key role in the analysis of the resilience of the network. Such an entity is assumed to be captured by a positive number $\xi \in (0, +\infty)$, and it grows – i.e., the effect of the shock becomes stronger – as the value of ξ increases.

The shock starts from a given node $i_0 \in V$ and propagates over the shortest paths with initial value i_0. More specifically, we do not prevent the shock to propagate over all the k-paths, but we do not consider the effects of the shock propagating outside the shortest paths. Practically, this means that the effect of the shock on a node connected to i_0 is registered only at the first time in which such a node is reached – thus, through the shortest path. After that, the node is infected, and it does not react to subsequent solicitations stemming from the same shock. The way propagation occurs depends on the weights of the shortest k-paths, on the entity of the shock and on the distance from the node subject to the shock.

According to [9], we consider the propagation on a generic k-path $p^{(k)}_{i_0}$ with weight as in (1) and define a discount factor $\delta \in [0, +\infty)$, that captures the effect of the distance on the propagation as follows

$$\xi_h = \xi \sum_{s=1}^{h} w_{i_{s-1} i_s} \delta^{h-s+1}, \tag{4}$$

where ξ_h is the entity of the shock at node i_h, for each $h = 0, \dots, k$ and $\xi_0 = \xi$.

We also include a propagation condition, which is the core of the resilience measure. Indeed, if the shock is too weak, then the propagation motion stops. To formalize the propagation condition, we introduce a vector $\Gamma = (\gamma_1, \dots \gamma_{\bar{k}}) \in (0, +\infty)^{\bar{k}}$ and assume that the existence of $s = 0, 1, 2, \dots, h-1$ such that $\xi_s < \gamma_s$ prevents the propagation of the shock to node i_h. The validity of the propagation conditions clusters the k-paths in two classes: the ones where the shock ξ propagates and those where such a shock does not achieve the last node. The clusters are, of course, dependent also on the considered vector Γ. We denote by $\mathcal{P}^{(k)}_{\Gamma,\xi}$ the set collecting the k-paths – not necessarily the shortest k-paths – which satisfy the propagation condition for Γ and ξ.

We are ready to define our concept of network resilience.

Given the vector Γ and the shock with entity ξ, we define the $\Gamma - \xi$-resilience measure of the network $N = (V, E)$ as

$$\mu_{(\Gamma,\xi)}(N) = 1 - \sum_{k=1}^{\bar{k}} \theta_k \frac{|\mathcal{P}^{(k)}_{\Gamma,\xi} \cap \mathcal{P}_{short}|}{|\mathcal{P}^{(k)} \cap \mathcal{P}_{short}|}, \tag{5}$$

where $\theta_1, \dots, \theta_{\bar{k}}$ are appropriately selected to be nonnegative weights such that $\sum_{k=1}^{\bar{k}} \theta_k = 1$. We denote the vector of the weights by $\Theta = (\theta_1, \dots, \theta_{\bar{k}})$. The selection of Θ is implemented on the basis of the specific attention towards the different lengths of the paths when measuring the resilience of the network.

We observe that $\mu_{(\Gamma,\xi)}(N) \in [0, 1]$ and it increases as the shocks propagate less easily over the network – so that, the network is more resilient. When $\mu_{(\Gamma,\xi)}(N) = 1$ ($\mu_{(\Gamma,\xi)}(N) = 0$, resp.), then the shock ξ is absorbed (the shock ξ propagates over all the paths, resp.).

2.1 Complexity test

The comparison between our proposal based on shortest paths and the approach of [9] – which takes into account all the paths – is associated to the discussion related to the complexity of the related algorithms. To face this relevant issue, we firstly provide a brief theoretical overview of the computational times in the two cases; then, we present an experiment supporting the theoretical side of the discussion.

The computation of all simple paths is well known to be a hard task [21], while the set of the shortest paths is easy to compute since the time complexity is polynomial in the size n of a graph G [4].

Table 1 shows the comparisons between the computation of $\mu_{(\Gamma,\xi)}(N)$ when considering all the simple paths (as in [9]) and when computing only the shortest paths according to Equation 5. The first column contains the type of network under examination, the second the cardinality of the set $\mathcal{P}^{(k)}$, the third the value for $\mu_{(\Gamma,\xi)}(N)$ and the fourth the computational time when computing all the simple paths. The following three columns show the same results when computing all the shortest paths and, finally, the last column reports the percentage deviation Δ_μ between the two values of $\mu_{(\Gamma,\xi)}(N)$. The simulations have been performed on ten instances with $\xi = 0.1$ and $\delta = 1$. All the values in Table 1 are to be considered averaged over ten instances.

Table 1 Result considering either the set of simple paths or the set of shortest paths in the $\mu_{(\Gamma,\xi)}(N)$ calculation for benchmark networks (averaged over 10 instances). In the Time columns, s are seconds, m are minutes, h are hours and d are days. In some rows results are not reported since the simulation ran out of memory after two days of computation.

	All simple paths			All shortest paths			
Network	$\lvert\mathcal{P}^{(k)}\rvert$	$\mu_{(\Gamma,\xi)}(N)$	Time	$\lvert\mathcal{P}^{(k)}\rvert$	$\mu_{(\Gamma,\xi)}(N)$	Time	Δ_μ
Grid, $n = 25$	185486.6	0.995	59.34 m	639.6	0.987	4.21 s	0.7%
Grid, $n = 50$	–	–	> 2 d	2632.3	0.990	10.57 s	–
Random, $n = 25$, $d = 0.1$	201.5	0.978	0.79 s	137.9	0.976	0.41 s	0.1%
Random, $n = 25$, $d = 0.2$	84980, 2	0.993	20.11 m	532, 3	0.984	2.03 s	0.9%
Random, $n = 50$, $d = 0.1$	–	–	> 2 d	2168.0	0.991	8.28 s	–
Random, $n = 50$, $d = 0.2$	–	–	> 2 d	2897.3	0.998	8.37 s	–

Since paths are the basic ingredient for our resilience measure, we followed the same general approach used in the analysis of shortest path problems [16] and we tested the two versions of the measure on grid and random networks. For both we considered $n = \{25, 50\}$ and w_{ij} randomly chosen in the set $\{1, 2, \ldots, 10\}$. Finally, in the case of random networks, we considered the values of density as $d = \{0.1, 0.2\}$.

From Table 1 we may notice that in all the simulations, as expected, the computational times for $\mu_{(\Gamma,\xi)}(N)$ considering all shortest paths outperform the other case. Note also that the gaps in the resilience measures Δ_μ are remarkably low (less than 1%), i.e. we can use the shortest paths at the cost of a small difference in the resilience measure.

It is worth noting that the negligible difference between the case of all paths and that of shortest paths was quite expected. Indeed, by definition, the shocks propagate more likely over the shortest paths than in the non shortest cases. In the considered situation, the percentage of the paths that are of non shortest nature and allowing the propagation of the shock is so small that the deviation between the resilience measures introduced in (5) and that in [9] is not that relevant.

3 The interbanking network model

The financial context here considered is taken from the interbanking system and data are retrieved by the BIS web site database [6]. In particular, we refer to the activities associated to the consolidated banking statistics (CBS) and to the Locational Banking Statistics (LBS) of all the available countries (see the details in the Appendix).

The CBS captures the worldwide consolidated positions of internationally active banking groups headquartered in reporting countries. The CBS include the business of banks' foreign affiliates but exclude intragroup positions, similarly to the consolidation approach followed by banking supervisors.

The LBS provide information about the currency composition of banks' balance sheets and the geographical distribution of their counterparties. The LBS capture the outstanding financial assets and liabilities of internationally active

banks located in reporting countries against counterparties residing in more than 200 countries[1].

The CBS and LBS data present different characteristics, even if they are associated to the same interbanking context. In our study, we consider the analysis conducted on LBS as a robustness check on the results obtained for CBS. We explain the reasoning behind this approach.

One of the reasons for preferring CBS is that consolidated statistics seems to be better suited for representing a risk-propagation scenario at aggregated level [39]. Moreover, taking into account the nationality of banks, rather than for instance their residency, could be deemed as a prudential way to involve countries in the process of risk propagation, especially considering the fact that BIS networks suffer of missing links by construction. Furthermore, consolidated data seem to be apt for research efforts that do not include an explicit geographical/spatial dimension as in our analysis.

Nonetheless, some authors argues that LBS display some advantages with respect to CBS such as available cross-border bank capital flows data, exchange rate adjusted flow data and a longer time window ([28], [29], [39]). For these reasons we repeat stress tests on the LBS dataset and compare it to the CBS dataset, in terms of our indicator μ, in order to understand whether the resilience displayed by CBS data is affected by the consolidation.

The considered datasets deal with banking groups in terms of hosting or residence countries, so that banks are intuitively associated to countries. Therefore, for both CBS and LBS networks, we take countries as nodes in the set $V = \{1, \dots, n\}$.

We assume that the weight w_{ij} is based on the aggregated bank exposures α_{ij} – expressed in billions of dollars – of the banking groups headquartered in country i to the ones of country j. Specifically, we consider $w_{ij} = \alpha_{ij}$, for each $i, j \in V$.

We present quarterly data, ranging from the first quarter of 2005 to the fourth quarter of 2020. Thus, we have 64 networks – one network for each quarter. The number of nodes and links varies over the periods: for CBS network, nodes range from 202 to 215 (210.05 on average) and links from 1922 to 2882 (2448.78 on average); for LBS networks, nodes range from 209 to 213 (211.72 on average) and links from 2688 to 4942 (3864.72 on average).

For the sake of completeness, consider that countries in the dataset are divided in three different classes [7]: i) the core, which considers the 26 reporting countries that have both incoming and outgoing exposure of international financial claims to the BIS (note that we report the actual number since countries have been added over the years); ii) the 10 global systemically (GS) countries where at least one G-SIB bank is headquartered[2]; iii) the periphery, which considers those countries where only inflow is available. Figures 1 and 2 show the network of the fourth quarter of 2020 for CBS and LBS, respectively, while Figures 3 and 4 illustrate the network of the GS elements in the same quarter for CBS and LBS, respectively.

Table 2 reported in Appendix shows the lists of core and GS countries. Such countries share a high number of links (see Figures 1–4 in both of cases of CBS

[1] Bank for International Settlements, Monetary and Economic Department, *Reporting guidelines for the BIS international banking statistics*, July 2019 (`https://www.bis.org/statistics/bankstatsguide.pdf`), accessed October 25^{th}, 2021.

[2] G-SIB banks (Global Systemically Important Banks) are subject to more stringent requirements. See `http://www.fsb.org/2017/11/fsb-publishes-2017-g-sib-list/` for the updated list of banks and requirements.

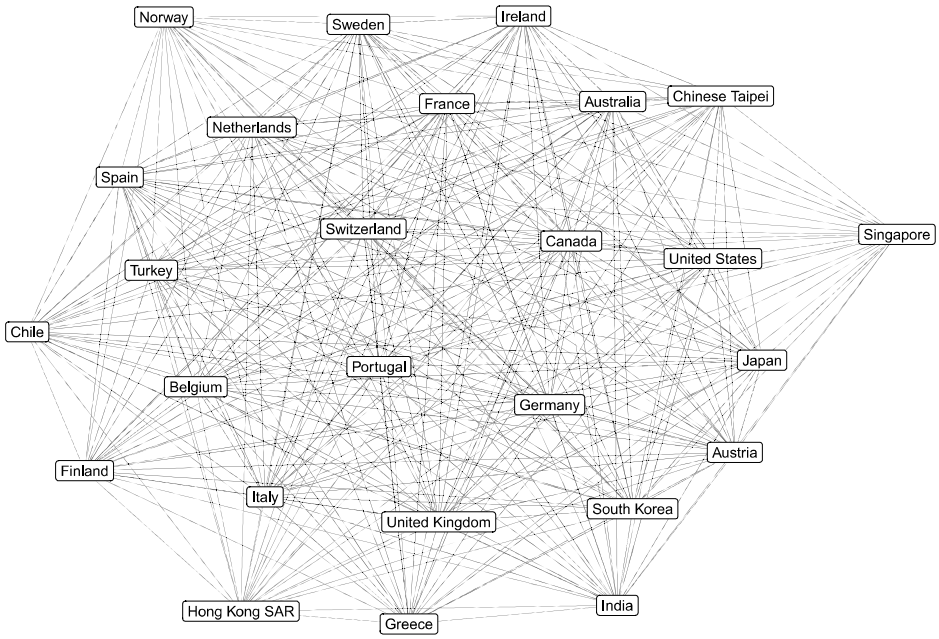

Fig. 1 Network of core elements (i.e. reporting countries) for the CBS fourth quarter of 2020. The existence of a link represents a positive cross-border exposure α_{ij} between the two nodes i, j.

and LBS and for a temporal instance), meaning that – under a purely topological perspective, i.e. in the unweighted case – the corresponding network structure has a local density considerably higher than the rest of the network. For this reason, the topological structure of the BIS networks is considered to be of core-periphery type.

Interestingly, in the case of core-periphery strucures, network resilience has some peculiar characteristics that are worth mentioning [12]. Indeed, in case of classical error and attack tolerance analysis, such networks are considered to be more resilient because of the presence of an high global cohesion, predominantly in the core. On the other hand, such networks are typically characterised by smaller values of the diameter, thus propagation towards other nodes is more likely to occur. Of course, the presence of the weights might lead to a departure of the weighted network from the topological core-periphery structure. However, the arguments above may be viewed as a support of the worthiness of our study.

In Figure 5 we show the in-degree and the out-degree distributions for CBS and LBS networks, respectively, as yearly boxplots, throughout the observation period. Implicitly, such distributions provide a confirmation of the topological core-periphery structure. Indeed, despite the shapes of the two distributions the values of y-axis differ due to the fact that – as already mentioned above – the peripheral countries report only inflow. We observe, with reference to the out-degree, a high number of banks/countries that do not have exchanges. This is due to the fact that the reporting countries make up a limited subset and some of

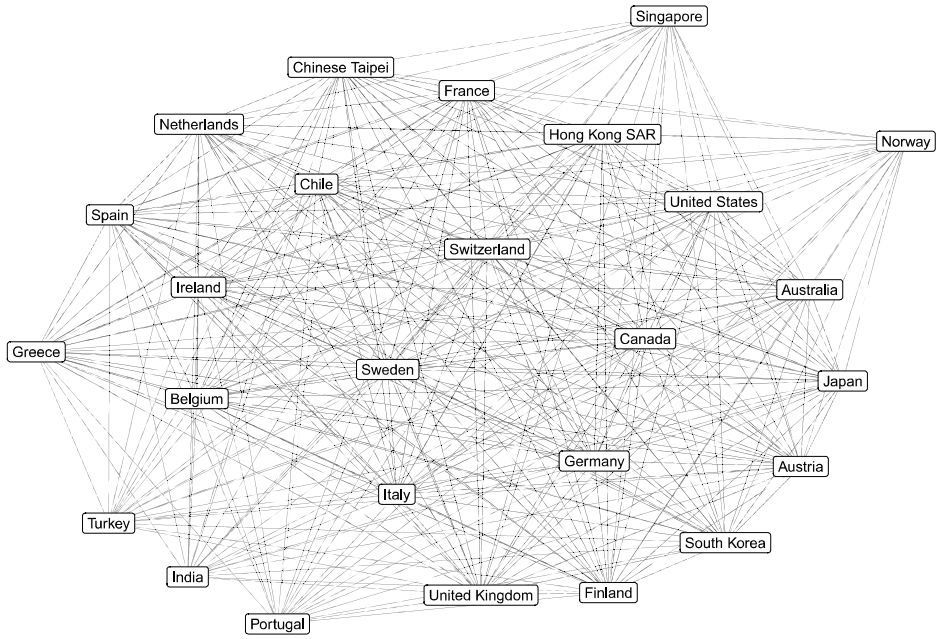

Fig. 2 Network of core elements (i.e. reporting countries) for the LBS fourth quarter of 2020. Also in this case, the existence of a link captures a positive cross-border exposure α_{ij} between the two nodes i, j.

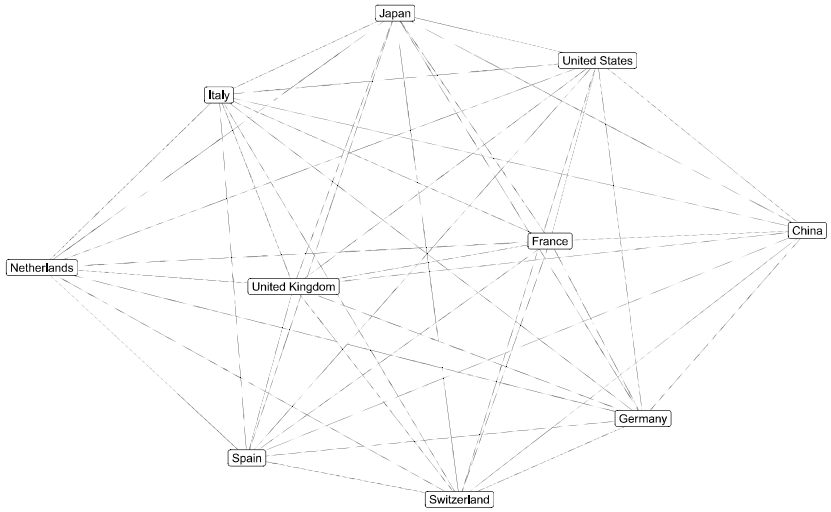

Fig. 3 Network of GS elements (i.e. countries where at least one global systemically important bank has its headquarter) for the CBS fourth quarter of 2020. Also in this case, the existence of a link captures a positive cross-border exposure α_{ij} between the two nodes i, j.

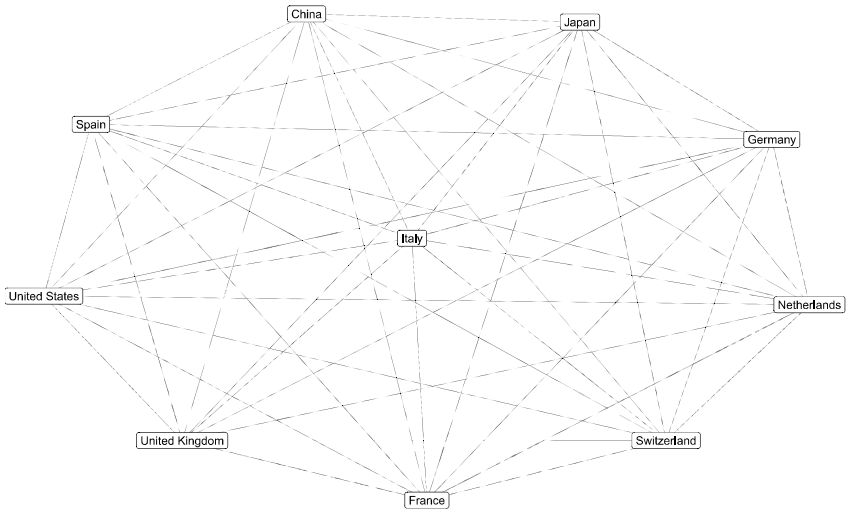

Fig. 4 Network of GS elements (i.e. countries where at least one global systemically important bank has its headquarter) for the LBS fourth quarter of 2020. Also in this case, the existence of a link captures a positive cross-border exposure α_{ij} between the two nodes i, j.

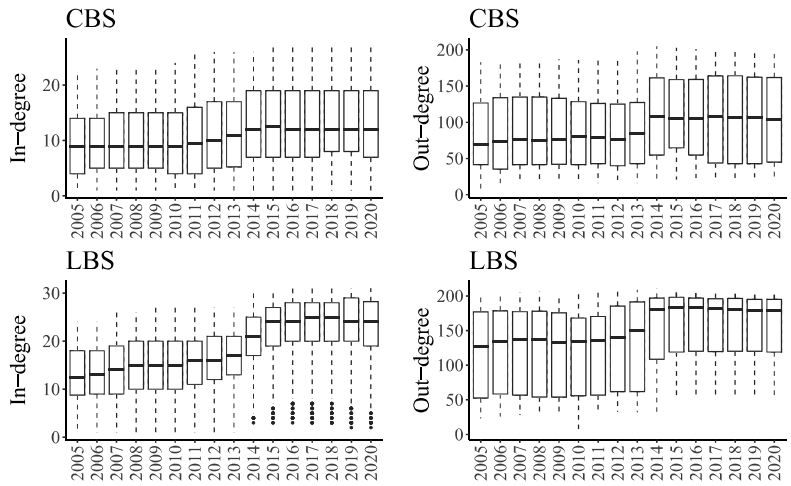

Fig. 5 Top panels: Yearly distributions of in-degree (left) and out-degree (right) for CBS networks. Bottom panels: Yearly distributions of in-degree (left) and out-degree (right) for LBS networks. In the out-degree distributions nodes with null out-degree values (peripheral elements) are filtered out.

the null values in the out-degree may be referred to the database incompleteness rather than to an absence of activity.

Finally, the out-degree shows remarkable fluctuations on the high values and data outlines the preferential exposure towards a limited number of banks/countries, with fluctuating exceptions.

4 Results and discussion

Herein we consider the analysis of the 64 BIS networks. They were built considering the CBS and LBS dataset fetched using the BIS API and cleaned from artifacts not regarding our purposes (e.g., rows containing summary data). The data processing, the network analysis and all simulations were conducted using the software *R* [35] with the *igraph* package [14].

Equation (5) has been implemented through an algorithm which takes the network N, the values of ξ and δ and of the components Γ and Θ as inputs.

Some scenarios for the values of ξ and δ and a peculiar setting for Γ and Θ are considered, to include a large number of cases in the analysis of the resilience. Specifically, we take $\xi_i = (w_{min} * 2^{10-i})^{-1}$ with w_{min} as the lowest link weight over all the 64 instances and $i = 1, 2, \ldots, 10$; thus, the parameter space is: for CBS networks $\xi \in \{0.0021, 0.0043, 0.0087, 0.0174, 0.03498, 0.0699, 0.1399, 0.2798, 0.5597, 1.1195\}$; for LBS $\xi \in \{0.0049, 0.0098, 0.0197, 0.0394, 0.0788, 0.1576, 0.3153, 0.6307, 1.2615, 2.5231\}$; and $\delta \in \{0.1, 0.25, 0.5, 0.75, 1, 2, 5, 10, 20, 50\}$. Summarising, we performed 100 computations for each of the CBS as well as for the LBS networks.

The highest values of ξ has been chosen in order to be greater than the diameter $\bar{k}$. Needless to say, $\bar{k}$ is taken as the maximum diameter of the 64 considered networks.

Regarding the setting for Γ and Θ, we considered $\Gamma = \{\gamma_i = 1, i = 1, ..., \bar{k}\}$ and $\Theta = \{\theta_i = 1/\bar{k}$, for $i = 1, \ldots, \bar{k}\}$. The former setting is associated to low propagation thresholds, so that a large number of shocks propagate. This condition can be seen as a prudential one, in that it avoids an a-priori mechanical removal of the effects of the shocks; the latter one considers uniform values of the θ's, hence leading to a fair evaluation of all the terms contributing in the definition of the resilience measure $\mu_{(\Gamma,\xi)}(N)$.

Figures 6-8 report the values of $\mu_{(\Gamma,\xi)}(N)$ for the CBS data, for every quarter and for each value of ξ, when considering all the values of δ, namely $\delta \in \{0.1, 0.25, 0.5, 0.75, 1, 2, 5, 10, 20, 50\}$. According to the selected values of δ, by merging the three figures we have ten panels.

As intuition suggests, we can generally say that the resilience of the networks decreases with respect to ξ. Indeed, by definition, a high value of the size ξ leads to an easier propagation of the shock.

We also notice the existence of a critical threshold of ξ above which we have the minimum level of resilience before year 2014 – the year following the Lehman Brothers failure and its consequences; this threshold reasonably decreases with respect to δ, so that a strong reduction of the shocks propagation over the paths – i.e., small values of δ – is associated to the propagation of shocks of large entity – i.e., shocks whose size is above the mentioned critical threshold.

Furthermore, the general level of the resilience measure decreases as δ increases. This outcome is due to the role of δ in the shock propagation process. Specifically, as δ increases, the propagation of the shock over a given path becomes more probable; thus, $|\mathcal{P}^{(k)}_{\Gamma,\xi} \cap \mathcal{P}_{short}|$ increases while $|\mathcal{P}^{(k)} \cap \mathcal{P}_{short}|$ remains constant, which implies that the resilience measure in (5) decreases.

In the extreme case of $\delta = 0.1$ – top-left panel in Figure 6 – the resilience attains values around the theoretical maximum for small values of ξ; moreover, the resilience surface does not show remarkable deviations across the years in this case. For high values of δ – more evidently in the bottom panels of Figure 7 and

Figure 8 – the resilience measure is close to zero for large values of ξ. This said, we observe a more scattered situation from 2017 to 2020, where one has traces of resilience – with resilience measure slightly greater than zero – also when $\xi = 10$. Interestingly, there is a resilience peak in 2008 when $\delta > 1$ – i.e., when the shock is amplified as the distance from the shocked node increases. This resilience peak is associated to the year of the Lehman Brothers' failure – hence, to the relevant global financial crisis related to this catastrophic event. Such an outcome can be explained by the amplification of the cohesiveness of the network in correspondence of the financial distress; this is in agreement with the stylized fact that economic actors are more correlated in situations of economic turmoil.

For average values of δ – see the bottom panels of Figure 6 and Figure 7 – we observe a collapse of the resilience measure in the triennium 2009–2012 – i.e., after the Lehman Brothers' failure. The relevance of such a collapse with respect to the adjacent years 2008 and 2013 is more evident for $0.5 \leq \delta \leq 5$. This is the period where the world experienced the consequences of the financial turmoil of 2008, with a lower level of interbanking exposures among countries that is associated to a lower capability of the network to absorb shocks in a post-financial crisis.

The turbulence of the financial world registered from 2014 – with the Russian and Chinese market crashes and the bad performance of the global stock markets in 2018 – is associated to the stronger interbanking relationships, hence leading to higher levels of the resilience measure after 2014. This argument is stressed in 2020 – i.e., in the dramatic socio-financial crisis generated by the COVID-19 pandemic – where we have the highest level of resilience, also in accord to the case of 2008.

Furthermore, we observe that the resilience of the network decreases with the value of δ. This outcome is in line with the role of the discount factor δ in the propagation of the shocks, and it represents a confirmation of the finding of our model. In this respect, the effect of δ on the resilience seems to be of remarkable relevance, mainly around the corner cases of $\delta = 0$ and $\delta = 1$. More interesting patterns are observed for fair values of δ – i.e., for $\delta = 0.4, 0.5$, see Figure 6. Indeed, in these cases, there is a collapse of the resilience around year 2014, after the period 2009-2013 of high resilience. The resilient period 2009-2013 corresponds to the one immediately following the Lehman Brothers' bankruptcy; hence, one can argue that the lowest level of interbanking exposures among countries is associated to a high capability of the network to absorb shocks in a post-financial crisis starting event period.

The results of the simulations of the LBS are reported in Figure 9-11. In general, we find a good agreement between the CBS and LBS across the parameter space, with the LBS networks slightly more resilient than the CBS ones and the flattening of the peaks in 2008 and 2020 in the LBS case. The robustness of the results is certified also by means of the Pearson's correlation between the time series of the indicator μ over CBS and LBS dataset for each value of δ and ξ – see Figure 12.

5 Conclusions

This paper proposes a novel resilience measure for networks that ranges in the unitary interval. Such a measure represents a relevant extension of the one proposed in [9]. In particular, the computational complexity of the original measure

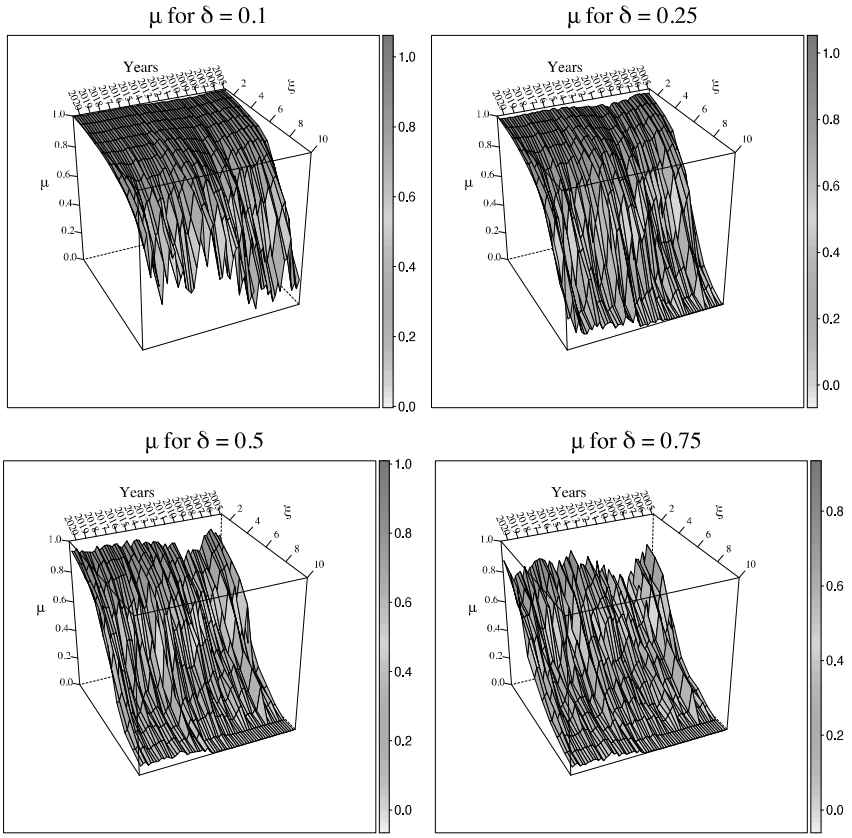

Fig. 6 Measures for the $\Gamma-\xi$-resilience $\mu_{(\Gamma,\xi)}(N)$ in the case of CBS networks for $\Gamma = \{\gamma_i = 1, i = 1, ..., \bar{k}\}$ and $\Theta = \{\theta_i = 1/\bar{k}$, for $i = 1, \ldots, \bar{k}\}$. Different values of ξ are reported on x-axis (as index of the vector), years on y-axis and values of $\mu_{(\Gamma,\xi)}(N)$ on z-axis. $(0.1 \leq \delta \leq 0.75)$.

has been removed by reasonably assuming – as in the cases of financial contagion – that shocks propagate over the shortest paths.

The introduced methodological device is tested over two meaningful networks built using the BIS database – with specific reference to the CBS data – of the interbank exposures gathered accordingly to the countries of the banks' headquarters. As robustness check, we also consider the networks built on the basis of the LBS data. The database is a precious source of information in that it provides evidence for the core-periphery structure of lending among banks worldwide, in line with previous results (see e.g. [13] or [26]). The considered model provides insights on the evolution of network resilience in different time periods. Several scenarios for the empirical analysis have been presented and discussed.

The dependence of the resilience on the size of the shock and on the presence of a distance-based mitigating/amplifying term of the propagation has been also detected. In so doing, the employed resilience measure represents – at least in the treated cases – is a suitable instrument for assessing the stability of the financial system. Importantly, the empirical experiments offer a resilience measure of the

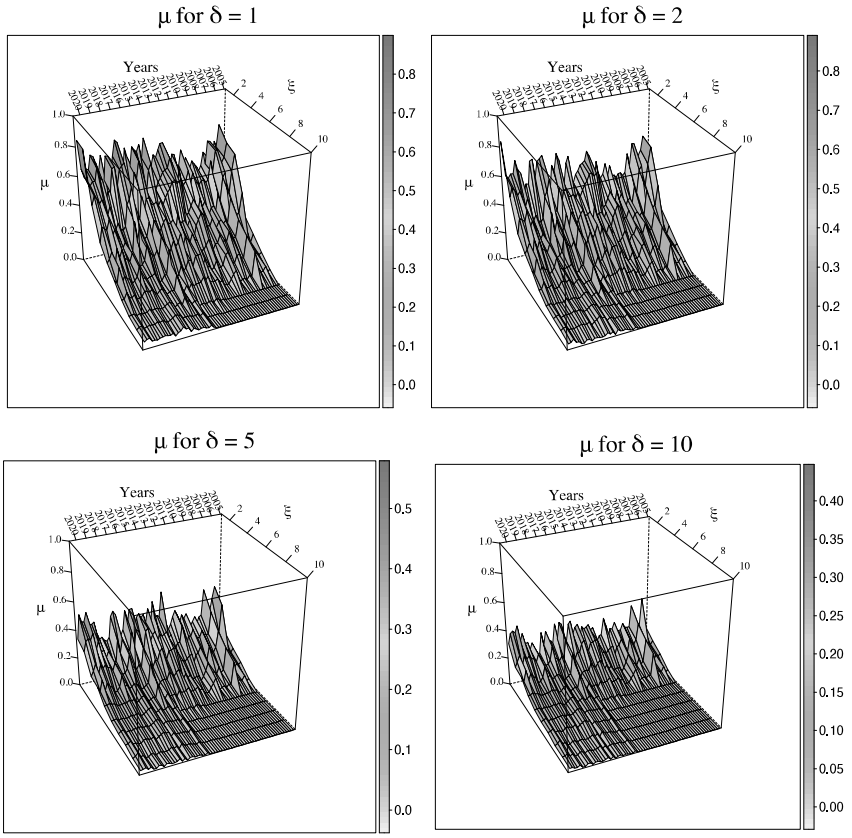

Fig. 7 Measures for the $\Gamma-\xi$-resilience $\mu_{(\Gamma,\xi)}(N)$ in the case of CBS networks for $\Gamma = \{\gamma_i = 1, i = 1, ..., \bar{k}\}$ and $\Theta = \{\theta_i = 1/\bar{k}$, for $i = 1, \ldots, \bar{k}\}$. Different values of ξ are reported on x-axis (as index of the vector), years on y-axis and values of $\mu_{(\Gamma,\xi)}(N)$ on z-axis. $(1 \leq \delta \leq 10)$.

BIS network which takes into full consideration some important financial crises of the 2000's, including the one started with the Lehman Brothers' failure in 2008 and the financial distress generated by the COVID-19 pandemic in 2020.

Results suggest that a high level of interbank exposures is able to immunize a system from the shocks in financial distress, while weakly interconnected banks generate a system of countries with a scarce attitude to absorb external shocks in presence of a financial turmoil. A possible interpretation of this outcome lies in the herd immunity against financial crisis of countries which are strongly linked through the banking system. Once such a link becomes weak enough, then the situation is reverted and countries are particularly sensitive to the contagion as financial distress appears.

Under a purely methodological perspective, the measure herein introduced can be considered also as a general tool that can be applied to networks belonging to other financial contexts for measuring systemic risk. This aspect opens the field for future applications in other financial domains. The analysis performed with our method could be also used in order to identify the features of the shocks which are

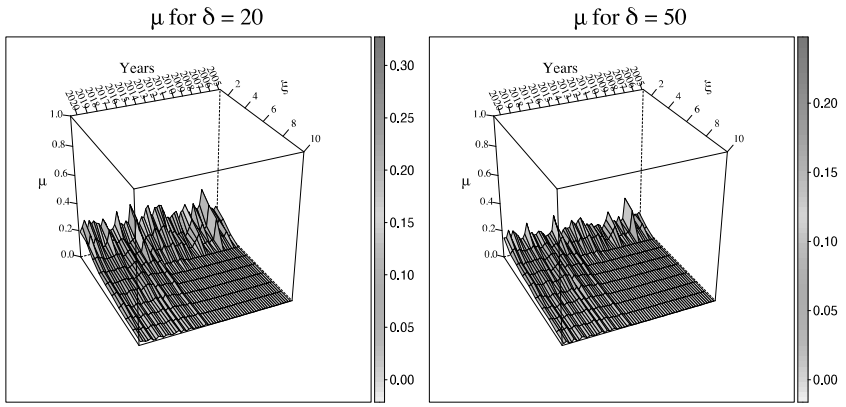

Fig. 8 Measures for the $\Gamma-\xi$-resilience $\mu_{(\Gamma,\xi)}(N)$ in the case of CBS networks for $\Gamma = \{\gamma_i = 1, i = 1, ..., \bar{k}\}$ and $\Theta = \{\theta_i = 1/\bar{k}$, for $i = 1, \ldots, \bar{k}\}$. Different values of ξ are reported on x-axis (as index of the vector), years on y-axis and values of $\mu_{(\Gamma,\xi)}(N)$ on z-axis. $(20 \leq \delta \leq 50)$.

correlated with the resilience of the network, possibly suggesting countermeasures in order to build more resilient financial systems.

References

1. Acemoglu, D., Ozdaglar, A., Tahbaz-Salehi, A., 2015. Systemic risk and stability in financial networks. *American Economic Review*, 105(2):564608.
2. Albert, R., Jeong, H. and Barabási, A-L. 2000. Error and attack tolerance of complex networks, *Nature*, 406:378–382.
3. Allen, F., and Babus, A. 2008. *Networks in finance*. Wharton Financial Institutions CenterWorking Paper No. 08-07.
4. Ahuja, R. K., Magnanti, T. L., Orlin, J. B., Network flows: Theory, Algorithms, and Applications, Pearson College Div (1988).
5. American Heritage Dictionary of the English Language, Fourth Edition, 2000.
6. BIS database `www.bis.org`.
7. Bongini, P., Clemente, G.P., Grassi, R., 2018. Interconnectedness, G-SIBs and network dynamics of global banking. *Finance Research Letters*, 27:185–192.
8. Cerqueti, R., Clemente, G.P., Grassi, R., 2020. Systemic risk assessment through high order clustering coefficient. *Annals of Operations Research*, doi:10.1007/s10479-020-03525-8.
9. Cerqueti, R., Ferraro, G., Iovanella, A., 2019. Measuring network resilience through connection patterns. *Reliability Engineering & System Safety*, 188:320–329.
10. Chen, P.Y. and Cheng, S.M. 2015. Sequential defence against random and intentional attacks in complex networks, *Physical Review E*, 91:022805(13).
11. Chevallier, J., Goutte, S., Guerreiro, D., Saglio, S., Sanhaji, B. (Eds.). (2019). International Financial Markets (Vol. 1). Routledge.
12. Cinelli, M., Ferraro, G., Iovanella, A., 2017. Resilience of core-periphery networks in the case of rich-club. *Complexity*, 2017:6548362.
13. Cinelli, M., Ferraro, G., Iovanella, A., Rotundo G. (2021). Assessing the impact of incomplete information on the resilience of financial networks, *Annals of Operations Research*, 299, 721–745.
14. Csardi G, Nepusz T. 2006. The igraph software package for complex network research. *InterJournal Complex System*, 1695. `http://igraph.org`.
15. D'Agostino, G., Scala, A., Zlatic, V. and Caldarelli, G. 2012. Robustness and assortativity for diffusion-like processes in scale-free networks. *Europhysics Letters*, 97(6):68006.
16. Demetrescu, C., Goldberg, A. V., Johnson, D. S. (Eds.), 2009. The shortest path problem: Ninth DIMACS implementation challenge (Vol. 74), *American Mathematical Soc.*.

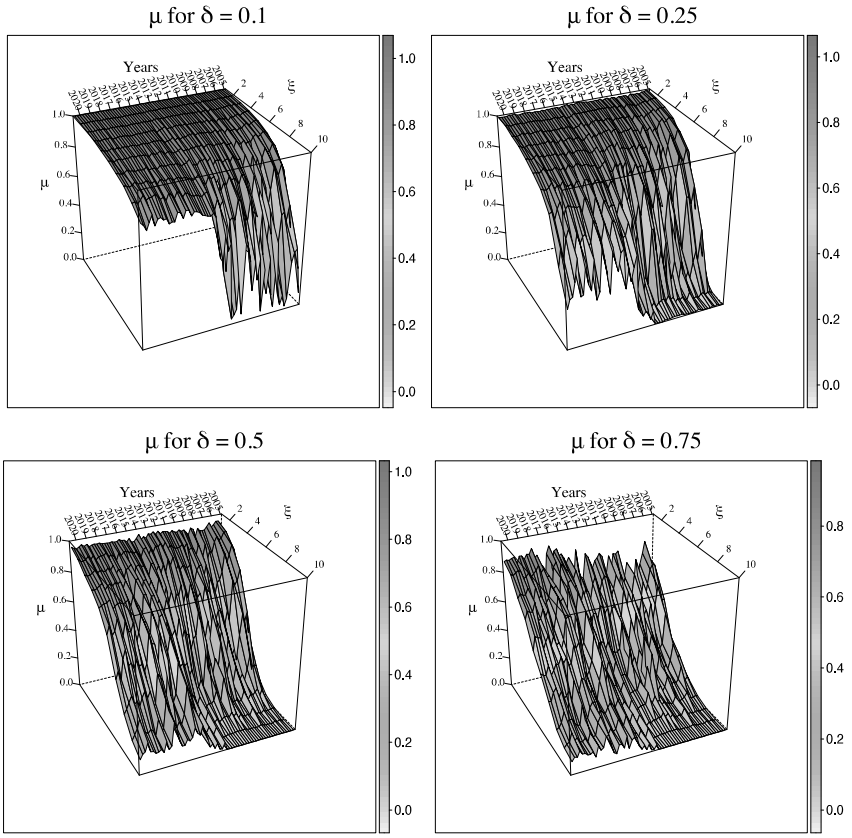

Fig. 9 Measures for the $\Gamma-\xi$-resilience $\mu_{(\Gamma,\xi)}(N)$ in the case of LBS networks for $\Gamma = \{\gamma_i = 1, i = 1, ..., \bar{k}\}$ and $\Theta = \{\theta_i = 1/\bar{k}$, for $i = 1, \ldots, \bar{k}\}$. Different values of ξ are reported on x-axis (as index of the vector), years on y-axis and values of $\mu_{(\Gamma,\xi)}(N)$ on z-axis. $(0.1 \leq \delta \leq 0.75)$.

17. Demir, M., Onder, Z., 2019. Financial connectivity and excessive liquidity: Benefit or risk? *Journal of International Financial Markets, Institutions and Money*, 62:203–221.
18. Dumontaux, N., Pop, A. 2013. Understanding the market reaction to shockwaves: evidence from the failure of Lehman Brothers. *Journal of Financial Stability*, 9(3):269–286.
19. Elliott, M., Golub, B. & Jackson, M. O. (2014). Financial Networks and Contagion. *American Economic Review* 104(10):3115–53.
20. Ferrraro, G., Iovanella, A. 2018. Clairvoyant targeted attack on complex networks. *International Journal of Computational Economics and Econometrics*, 8(1):41-62.
21. Fortune S, Hopcroft JE, Wyllie J. 1980. The directed subgraph homeomorphism problem. *Theoretical Computer Science*, 10:111–21.
22. Gao, J., Barzel, B. and Barabási, A-L. 2016. Universal resilience patterns in complex networks. *Nature*, 530(7590):307-312.
23. Giudici, P., Spelta, A 2016. Graphical network models for international financial flows. *Journal of Business & Economic Statistics*, 34(1):128-138.
24. Glasserman, P. & Peyton Young, H. (2016). Contagion in Financial Networks. *Journal of Economic Literature*, 54(3):779-831.
25. Huang, Y.-P., Hsu, C.-C., and Wang, S–H. 2007. Pattern recognition in time series database: A case study on financial database. *Expert Systems with Applications*, 33(1):199-205.

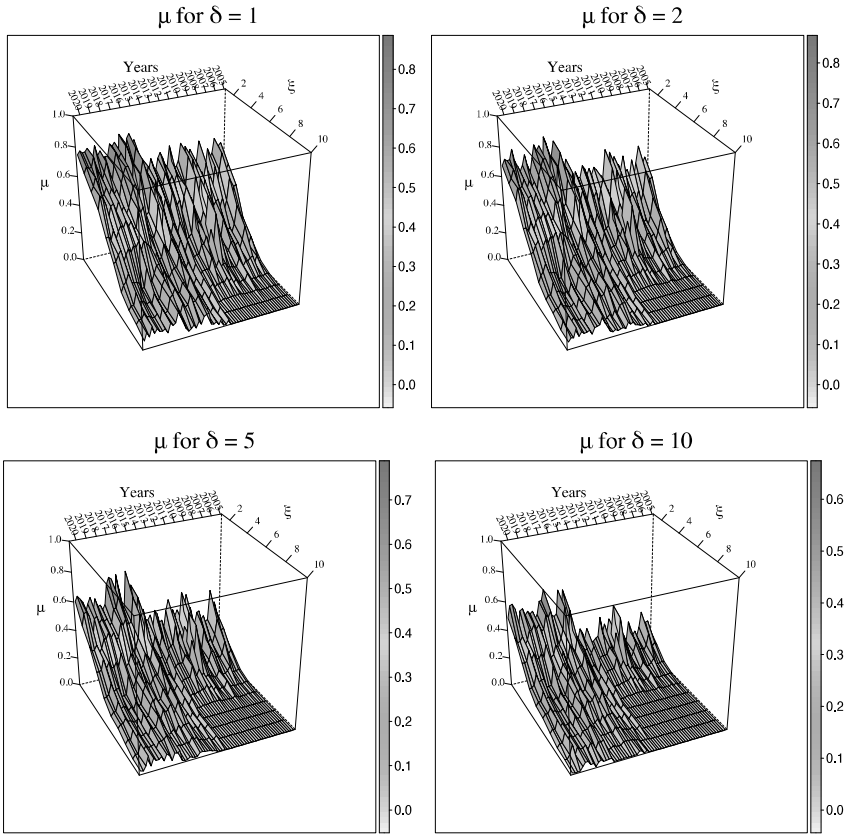

Fig. 10 Measures for the $\Gamma-\xi$-resilience $\mu_{(\Gamma,\xi)}(N)$ in the case of LBS networks for $\Gamma = \{\gamma_i = 1, i = 1, ..., \bar{k}\}$ and $\Theta = \{\theta_i = 1/\bar{k}$, for $i = 1, \ldots, \bar{k}\}$. Different values of ξ are reported on x-axis (as index of the vector), years on y-axis and values of $\mu_{(\Gamma,\xi)}(N)$ on z-axis. $(1 \leq \delta \leq 10)$.

26. Kojaku, S., Cimini, G., Caldarelli, G. & Masuda, N., 2018. Structural changes in the interbank market across the financial crisis from multiple core-periphery analysis *Journal of Network Theory in Finance*, 4(3):33-51.
27. Iyer, S., Killingback, T., Sundaram, B. and Wang, Z. 2013. Attack robustness and centrality of complex networks. *PLoS ONE*, 8(4):e59613.
28. Minoiu, C., Kang, C., Subrahmanian, V., Berea, A., 2015. Does financial connectedness predict crises? *Quantitative Finance*, 15:607-624.
29. Minoiu, C., Reyes, J.A., 2013. A network analysis of global banking: 1978-2010. *Journal of Financial Stability*, 9(2):168–184.
30. Nagurney, A., and Ke, K. 2006. Financial networks with intermediation: Risk management with variable weights. *European Journal of Operation Research*, 172:40–63.
31. Nagurney, A., and Siokos, S. 1998. Network modeling of international financial equilibria with hedging. *Annals of Operation Research*, 82:139–160.
32. Nedovic, L., and Devedzic, V. 2002. Expert systems in finance - A cross-section of the field. *Expert Systems with Applications*, 23(1):49–66.
33. Peron, T.K., Costa, L.d.a. F. and Rodrigues, F.A. (2012). The structure and resilience of financial market networks. *Chaos*, 22:013117.
34. Rada, R., 2008. Expert systems and evolutionary computing for financial investing: A review. *Expert systems with applications*, 34(4):2232–2240.
35. R Core Team. R: A language and environment for statistical computing. *R Foundation for Statistical Computing*, Vienna, Austria 2014. http://www.R-project.org.

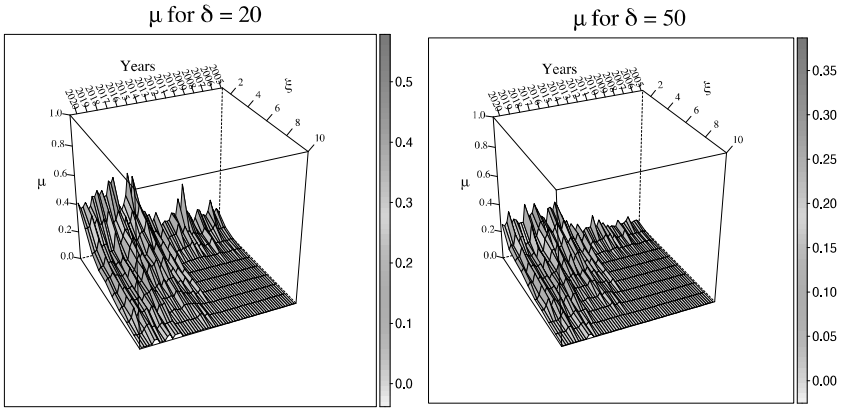

Fig. 11 Measures for the $\Gamma-\xi$-resilience $\mu_{(\Gamma,\xi)}(N)$ in the case of LBS networks for $\Gamma = \{\gamma_i = 1, i = 1, ..., \bar{k}\}$ and $\Theta = \{\theta_i = 1/\bar{k}$, for $i = 1, \ldots, \bar{k}\}$. Different values of ξ are reported on x-axis (as index of the vector), years on y-axis and values of $\mu_{(\Gamma,\xi)}(N)$ on z-axis. $(20 \leq \delta \leq 50)$.

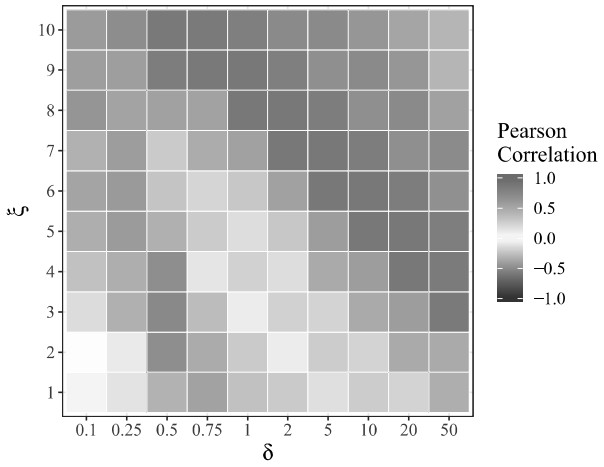

Fig. 12 Correlation matrix between the time series (ranging in each period from 2005 to 2020) of μ computed using CBS and LBS data across the parameter space. Since the parameter ξ is a function of w_{min} we considered its rank values.

36. Rosas-Casals, M., Bologna, S., Bompard, E. F., D'Agostino, G., Ellens, W., Pagani, G. A., ... & Verma, T. 2015. Knowing power grids and understanding complexity science. *International Journal of Critical Infrastructures*, 11(1):4-14.
37. Scala, A., Lucentini, P. G. D. S., Caldarelli, G.,& D'Agostino, G. 2016. Cascades in interdependent flow networks. *Physica D: Nonlinear Phenomena*, 323:35-39.
38. Sensoy, A., Nguyen, D.K., Rostom, A. and Hacihasanoglu, E. (2019). Dynamic integration and network structure of the EMU sovereign bond markets. *Annals of Operations Research*, 281 (12):297-314.
39. Tonzer, L. (2015). Cross-border interbank networks, banking risk and contagion. *Journal of Financial Stability*, 18:19-32.
40. Zhu, Y., Yang, F. & Ye, W. (2018) Financial contagion behavior analysis based on complex network approach *Annals of Operation Research*, 268:93-111.

Appendix: BIS description

BIS database is owned by 60 central banks, which cover about 95% of the world's GDP. The role of BIS is to provide a rigorous statistical description of international markets and financial intermediaries.

The available reporting countries – which are also those considered in the present study – are Australia, Austria, Belgium, Brazil, Canada, Chile, Chinese Taipei, Denmark, Finland, France, Germany, Greece, Hong Kong SAR, India, Ireland, Italy, Japan, Luxembourg, Mexico, Netherlands, Norway, Panama, Portugal, Singapore, South Korea, South Korea, Spain, Sweden, Switzerland, Turkey, United Kingdom, United States.

The counterpart countries are: Afghanistan, Albania, Algeria, Andorra, Angola, Argentina, Armenia, Aruba, Azerbaijan, Bahamas, Bahrain, Bangladesh, Barbados, Belarus, Belize, Benin, Bermuda, Bhutan, Bolivia, Bonaire, Sint Eustatius and Saba, Bosnia and Herzegovina, Botswana, Brunei, Bulgaria, Burkina Faso, Burundi, Cambodia, Cameroon, Cape Verde, Cayman Islands, Central African Republic, Chad, China, Colombia, Comoros, Congo, Congo Democratic Republic, Costa Rica, Cote d'Ivoire, Croatia, Cuba, Curacao, Cyprus, Czech Republic, Czechoslovakia, Djibouti, Dominica, Dominican Republic, Ecuador, Egypt, El Salvador, Equatorial Guinea, Eritrea, Estonia, Ethiopia, Faeroe Islands, Falkland Islands, Fiji, French Polynesia, Gabon, Gambia, Georgia, German Democratic Republic, Ghana, Gibraltar, Greenland, Grenada, Guatemala, Guernsey, Guinea, Guinea-Bissau, Guyana, Haiti, Honduras, Hungary, Iceland, Indonesia, Iran, Iraq, Isle of Man, Israel, Jamaica, Jersey, Jordan, Kazakhstan, Kenya, Kiribati, Kuwait, Kyrgyz Republic, Laos, Latvia, Lebanon, Lesotho, Liberia, Libya, Liechtenstein, Lithuania, Macao SAR, Macedonia (FYR), Madagascar, Malawi, Malaysia, Maldives, Mali, Malta, Marshall Islands, Mauritania, Mauritius, Micronesia, Moldova, Mongolia, Montenegro Morocco, Mozambique, Myanmar, Nauru, Nepal, Netherlands Antilles, New Caledonia, New Zealand, Nicaragua, Nigeria, North Korea, Oman, Pakistan, Palau, Palestinian Territory, Papua New Guinea, Paraguay, Peru, Philippines, Poland, Qatar, Romania, Russia Rwanda, Samoa, San Marino, Sao Tome and Principe, Saudi Arabia, Senegal, Serbia, Serbia and Montenegro, Seychelles, Sierra Leone, Sint Maarten, Slovakia, Slovenia, Solomon Islands, Somalia, South Africa, South Sudan, Soviet Union, Sri Lanka, St. Helena and Dependencies, St. Lucia, St. Vincent and the Grenadines, Sudan, Suriname, Swaziland, Syria, Tajikistan, Tanzania, Thailand, Timor Leste, Togo, Tonga, Trinidad and Tobago, Tunisia, Turkmenistan, Turks and Caicos Islands, Tuvalu, Uganda, Ukraine, United Arab Emirates, Uruguay, US Pacific Islands, Uzbekistan, Vanuatu, Vatican City State, Venezuela, Vietnam, Wallis and Futuna, Yemen, Yugoslavia, Zambia, Zimbabwe.

Countries belong to three different groups (see [7]): 26 core countries, which report to the BIS both outgoing and incoming exposures to the BIS; 10 Global Systemically (GS) countries, each of them being the headquarter of at least one Global Systemically Important Banks (G-SIB). Such banks have to obey more stringent requirements in reporting their data (see `http://www.fsb.org/2017/11/fsb-publishes-2017-g-sib-list/`; data on core and GS have been included also in Table 2); the peripheral countries, for which only the inflows are available.

Table 2 List of core countries in 2020. Some of them form also the group of GS countries, as indicated.

Australia (AU)	Core	
Austria (AT)	Core	
Belgium (BE)	Core	
Canada (CA)	Core	
Chile (CL)	Core	
China (CN)		GS
Chinese Taipei (TW)	Core	
Finland (FI)	Core	
France (FR)	Core	GS
Germany (DE)	Core	GS
Greece (GR)	Core	
Hong Kong SAR (HK)	Core	
India (IN)	Core	
Ireland (IE)	Core	
Italy (IT)	Core	GS
Japan (JP)	Core	GS
South Korea (KR)	Core	
Netherlands (NL)	Core	GS
Norway (NO)	Core	
Portugal (PT)	Core	
Singapore (SG)	Core	
Spain (ES)	Core	GS
Sweden (SE)	Core	
Switzerland (CH)	Core	GS
Turkey (TR)	Core	
United Kingdom (GB)	Core	GS
United States (US)	Core	GS